Proceedings of the 3rd IASME/WSEAS Int. Conf. on HEAT TRANSFER, THERMAL ENGINEERING AND ENVIRONMENT, Corfu, Greece, August 20-22, 2005 (pp122-127)

Steady and unsteady natural circulation in a single-phase 2D-annular loop

Gilles DESRAYAUD[1], Alberto FICHERA[2] and Manuel MARCOUX[1]
[1]INSSET/LETEM, Université de Picardie Jules Verne
48 rue Raspail BP 422 02109 Saint-Quentin FRANCE
[2]Dipartimento di Ingegneria Industriale e Meccanica, Università di Catania
Viale A. Doria 6 95125 Catania ITALY

Abstract: - In this study, natural convection in a 2D-annular closed-loop thermosyphon filled with water is numerically investigated. The loop is heated at a constant flux over the bottom half and cooled at a constant temperature over the top half. It is numerically demonstrated that the complexity of the dynamic properties experimentally encountered in loops is also found here: steady flow with and without recirculating regions, periodic motion and Lorenz-like chaotic flow. The present numerical experiment also corroborates the fact that forced flow correlations are assumed to be applicable for natural circulation flow. The dimensionless group, $Gr_m(D_h/L)$, proposed by Vijayan and Austregesilo [13] for the mass flow rate gives very good results in the case of annular loop even for various Prandtl numbers.

Key-Words: - **Natural circulation, 2D-annular loop, Numerical simulation, Reynolds correlation**

1 Introduction

Natural circulation loops are systems in which the flow is driven by buoyancy forces created by heating and cooling of a fluid inside a torus placed in a vertical plane so that pumping is not required. This device is a type of thermosyphon, a non-mechanical heat pump used for cooling purposes in industrial processes, including solar water heaters, geothermal processes, gas turbine blade cooling, and as part of the emergency core cooling system in nuclear reactors. Because of their practical importance, thermosyphons have been the subject of a large number of theoretical and experimental studies. A review of the wide applications of natural circulation loops in engineering systems has been given by Zvirin [15]. These also attract attention because of the variety of fluid motions and the complexity of the dynamic properties encountered, in spite of the simplicity of their geometry. The research pioneered by Keller [8], Welander [14] and Malkus [10] has been reviewed by Greif [6]. The presence of a reverse flow region was first qualitatively reported by Creveling et al. [3] who also first observed the Lorenz-like chaotic flow in their experiments (see also [5, 11]).

Previous studies of toroidal loops have utilized a one-dimensional approach by averaging the governing equations over the pipe cross-section, which required a priori specifications of the friction and the heat transfer coefficients. Conventional forced flow correlations for fully developed flow are usually assumed to be applicable to natural circulation flow in 1D analyses. It is also assumed that the velocity is solely in the axial direction and that the effects of the pipe curvature and axial conduction are negligible. Integrating the momentum equation around the loop reduces this equation to an overall balance between buoyancy and friction.

To our knowledge, no direct unsteady 2D numerical simulations exist in the literature and only one numerical experiment on steady 3D flow in a toroidal loop can be found (Lavine et al., [9]).

The purpose of the present study is to investigate by direct numerical integration of the governing equations, the steady and unsteady motions in a thermosyphon of simple well-defined geometry, a 2D-annular loop.

2 Analysis and numerical resolution

Consider a 2D-annular loop of laminar fluid heated over one-half its area at a uniform heat flux (q") and cooled over the remaining half at a constant temperature (T_c) as shown in Fig. 1. The inner (respectively outer) cylinder radius is r_i^* (resp., r_o^*), the channel gap being defined as, $a = r_o^* - r_i^*$. The classical governing (Navier-Stokes plus energy) equations for incompressible fluid with the Boussinesq approximation used in cylindrical coordinates, are not written here due to lack of space but can be found in Desrayaud et al. [4]. The way in which the equations are non-dimensionalized are the following for the dimension, time, velocity and temperature:

$$r = \frac{r^* - r_i^*}{a} \quad \tau = \frac{\alpha t^*}{a^2} \quad u = \frac{a u^*}{\alpha} \quad \Theta = \frac{T - T_c}{\Delta T} \quad \Delta T = \frac{a q''}{\kappa} \qquad (1)$$

The thermo-physical characteristics of the fluid are its thermal diffusivity α, its kinematic viscosity ν and its thermal conductivity κ. β is the coefficient of thermal expansion and the non-dimensional radial and axial velocity are u and v.

The non-dimensional boundary conditions are the following, the angular coordinate θ being measured from the downward vertical (Fig. 1):

Heating section at $-\pi/2 \le \theta \le \pi/2$, r = 0 and 1

$$u = v = 0 \qquad \frac{\partial \Theta}{\partial r} = -1 \qquad (2a)$$

Cooling section at $\pi/2 \le \theta \le 3\pi/2$, r = 0 and 1

$$u = v = 0 \qquad \Theta = 0 \qquad (2b)$$

2π-periodicity in the θ direction $0 < r < 1$,

$$u, v, \Theta\big|_{\theta=0} = u, v, \Theta\big|_{\theta=2\pi} \qquad (2c)$$

The motionless and isothermal solution used as the initial guess for computations is given by,

for $\tau = 0$ at $0 \le r \le 1$ and $0 \le \theta \le 2\pi$, $u = v = 0$ $\Theta = 0$ (3)

The non-dimensional parameters that govern the flow are the Rayleigh number Ra build on **a** (or Ra_{2a} build on the hydraulic diameter, $D_h = 2a$), the Prandtl number Pr and the radius ratio R which are defined by

$$Ra = g\beta a^3 \Delta T/\alpha\nu \ (= Ra_{2a}/8) \quad Pr = \nu/\alpha \quad R = r_o^*/r_i^* \qquad (4)$$

The control volume procedure is utilized to discretize on a staggered, uniform cylindrical grid the non-linear system of governing equations and boundary conditions with the second order centered scheme for the convective terms. The SIMPLER algorithm is employed to solve the coupling between continuity and momentum equations through pressure. All the conservation equations were cast in transient form with a semi-implicit scheme for temporal integration (ADI method). A uniform grid with 30*x*320 control volumes in the r and θ directions was used to obtain all the results presented in this paper. This computational code was also used by Cadiou et al. [1] and validated on several cases.

The Fanning friction factor f_F on the inner and outer walls is calculated as

$$f_F = -\frac{\mu\, r^* \dfrac{\partial}{\partial r^*}\left(\dfrac{v^*}{r^*}\right)\Big|_w}{\dfrac{1}{2}\rho \overline{V}^{*2}} \qquad (5)$$

$\overline{V}^*$ being the dimensional cross-sectional average velocity.

For forced laminar flow in a planewall channel, the Fanning friction factor can be analytically calculated and is equal to $24/Re_{2a}$, the Reynolds number being based on the hydraulic diameter 2a and equal to $Re_{2a} = \dfrac{\rho \overline{V}^{*2} 2a}{\mu}$

3 Results

Results shown here are for radius ratio, R = 2.0 but calculations were also carried out for other radius ratios R = 1.08, 1.2, 1.4, 1.6, 1.8 and the trend presented can be extended to these. The working fluid was water with Prandtl number, Pr = 5, in all cases. Over 100 runs have been carried out for steady flows and 50 for unsteady flows.

3.1 Steady flow

At very low values of the Rayleigh number (Ra = 1 for example), the global motion all around the loop is almost inexistent and two very large re-circulations of weak motion occur (not shown here). Due to the symmetry of the heating and cooling sections to the vertical axis, the flow can be clockwise or counter-clockwise by chance. The stratified temperature which is symmetrically distributed in both halves of the annulus ([0,-π] and [0, π] Fig. 2) reveals the importance of the axial conduction, the convection playing only a minor role in the heat transfer. Hence, heat being mainly transferred by conduction from the lower hot part to the upper cold part, this regime can be appropriately qualified as pseudo-conductive. It should be noted that a purely conductive solution was never found (i.e., with no fluid motion). Two convective solutions of very weak motion branch off symmetrically from the state of rest (i.e., Ra = 0) undergoing a pitchfork bifurcation [4].

For moderate values of the Rayleigh number, a quasi-one-dimensional flow exists along the loop and the flow is steady without undergoing any oscillatory process. With increase in Ra, the fluid flow undergoes a short time oscillation before becoming stable. The temperature, stream function and axial velocity fields for Ra = 10 000 and R = 2.0 are shown in Fig. 3, the fluid moving around the loop in a counter-clockwise direction. A zone of very strong temperature increase is clearly visible at the entrance of the heater along the outer wall (Fig. 3a, arrow (1)). On the other hand, this phenomenon does not exist at the cooler entrance due to the imposed temperature at the walls (Fig. 3a, arrow (2)). The streamlines that were concentric for low values of the Rayleigh number are now slightly deformed at the entrance region of the exchangers, the streamlines being more distorted at the heater (Fig. 3b). At Ra = 13 500 (Fig. 4), it should be noted that, in addition to the circulatory main flow, two cells in the second and in the fourth quadrant can be seen. These two recirculating regions occur near the outer wall of the entrance of the heat exchangers (Fig. 4b,c), the bigger vortex always being at the heater while the one at the cooler is very weak. As a consequence, the zone of the strong temperature increase that extended largely downstream along the outer walls is now reduced (Fig. 4a, arrow (1)). These cellular structures appear at values of the Rayleigh number close to 13 800 which represents the upper limit of the steady motion.

The dimensionless temperatures at the inner and outer wall are shown in Fig. 5a only along the heater, the

cooler being at an imposed temperature. The temperature of the outer wall is always largely greater than the temperature of the inner wall. This is due to the boundary condition, imposed heat flux at the heater, combined with the curvature. Since the surface of the outer wall is R times greater than the surface of the inner wall, the total heat flux transferred to the convective fluid flow is also R times greater and there results a higher level of temperature at the outer wall. At Ra = 10 000, the average temperature of the outer wall is $\overline{\Theta}_h = 0.535$ while it is only 0.387 at the inner wall. The temperature increase at the outer wall is clearly seen at Ra = 10 000 (Fig. 5a) followed by a plateau. This can explains why the fluid is able to proceed upstream along the outer wall at the entrance of the heat exchanger. At Ra = 13 500, inverse temperature stratification occurs (Fig. 5a) that causes this very large recirculation at the entrance of the heater (Fig. 4b).

The sum of the local inner and outer wall friction factor is given in Fig. 5b as a function of θ. The two peaks of the friction factor curves correspond to the exit of the exchangers while at the entrance $f_F\,Re_{2a}$ drops significantly. Surprisingly, this trend is smaller at the heater entrance than at the cooler entrance where $f_F\,Re_{2a}$ becomes negative (Ra = 13 500). This is due to the small recirculation at the outer wall of the cooler entrance (with low axial velocity and consequently low friction). At the inner wall, near $\theta = \pi/2$, the motion slows down and a detachment is close to occurring (but does not occur, see Figs. 3c and 4c, arrow (3)).

3.2 Periodically oscillatory flow

Some authors have shown analytically and confirmed experimentally that steady flow is not achievable in a closed loop thermosyphon for a certain range of heat inputs. In the present study, for Rayleigh numbers greater than 13 800, the flow first begins to oscillate periodically with a constant amplitude of very small magnitude. The system is attracted to a limit cycle clearly illustrated in Fig. 6 (Ra = 13 830). The phase portrait of $[\Theta(0.5,0), \Theta(0.5,\pi/2)]$ is for every time step during the time interval [0,10] representing almost 60 cycles with 830 iterations per cycle. During the periodic motion, the two cells oscillate on the spot, their strength (and size) varying slightly. The limit cycle clearly indicates that the motion is periodic with one frequency, $f = 5.76 \pm 0.10$.

For smaller radius ratios, the Rayleigh numbers at which recirculating regions and oscillatory flow phenomena occur increase. For instance, oscillatory flow occurs at approximately Ra = 23 500 (respectively, 120 000) for R =1.6 (resp., 1.2).

3.3 Reverse flow and Lorenz-like attractor

For Rayleigh numbers greater than 15 000, unstable flow occurs and the flow rate oscillates with increasing amplitude until it eventually reverses direction, whereupon oscillations initiate in a new flow direction. Figure 7a presents the time history of the stream function at the middle of the cooler $(0.5, \pi)$. This variable clearly indicates the changes of flow direction with its change of sign. Compared to Fig. 4, the positions of the two cells are irregularly shifted to the first and third quadrant of the loop. Several experiments on the thermal convection in a closed loop have been made and some of their results show Lorenz-like behavior [2, 3, 11] as in the present numerical experiment, Fig. 7b showing the recognizable shape of the Lorenz attractor. This phase portrait has been built with only one time series (horizontal axis), that of the stream function given in Fig. 7a and using a time step lag of $\Delta\tau = 0.03$ for the other one (vertical axis).

3.4 Reynolds correlation

Recently, Vijayan [12, 13] demonstrated, that for the steady state behavior of natural circulation loop, it is only necessary to simulate a single non-dimensional parameter which is non-loop specific, namely, $Gr_m\,(D_h/L)$. They carried out experiments in three rectangular, natural circulation loops of different pipe diameters. They succeeded in developing scaling laws for single-phase natural circulation loops based on these experiments, and using a simple 1D analysis as did Zvirin [15]. Surprisingly, when accounting for local pressure losses, their results showed that secondary flows and the fact that flow is undeveloped are of small importance, as evidenced by a comparison of their generalized correlation against data of uniform and non-uniform diameter loops [12]. Moreover, in the calculation of the overall loss coefficient, they used the conventional forced flow correlation for friction factor and took into account the loss coefficients if they were significant. The generalized correlation is in good agreement with the experimental data of Huang and Zelaya [7] who were the only ones to account for the local pressure losses. The numerical friction factor has been calculated using eq. (5) and gives results which are very closed to the analytical value. Over more than 100 runs, it has been numerically found that $f_F\,Re_{2a} = 23.15 \pm 0.84$ while the analytical value is 24. It can be concluded that the friction factor is neither greatly affected by recirculation nor by curvature effect and that conventional forced flow correlation can be used for

natural circulation loop. The present conclusion is due to the absence of pressure losses due to the presence of bends and flow area changes in the annular loop.

Figure 8 shows the steady state mass flow rate from various uniform gap widths of an annular loop as a function of the non-dimensional group $Gr_m (D_h/L)$. Gr_m is the modified Grashof number introduced by Vijayan and Austregesilo [13] and D_h is the hydraulic diameter. The non-dimensional group is defined using the present symbols by:

$$Gr_m \left(\frac{D_h}{L}\right) = \frac{Ra_{2a}}{Pr^2}\frac{R+1}{R-1} \qquad (6)$$

Using the theoretical correlation of the Fanning friction factor for fully developed forced flow in a plane wall channel for laminar flow, $f_F = \frac{p}{Re_{2a}^b} = \frac{24}{Re_{2a}}$, the proposed correlation of Vijayan [12] can thus be expressed as

$$Re_{2a} = \left(\frac{8}{p}\right)^{1/(3-b)} \left(Gr_m \frac{D_h}{L}\right)^{1/(3-b)} = 0.144 \left(\frac{Ra_{2a}}{Pr^2}\frac{R+1}{R-1}\right)^{0.5} \qquad (7)$$

The numerical data are adequately represented by the theoretical correlation (Fig. 8) except at very low values, for which small deviations can be seen, the regime being pseudo-conductive.

The Reynolds correlation has also been validated vs the Prandtl number dependence. To do this, some extra computations have been performed for three different values of the Prandtl number, 1, 20, 50 and for one given radius ratio, R = 1.60. The accuracy is very good. Other results at R = 2.00 can be found in [4].

4 Conclusion

The behavior of a natural circulation loop that is heated uniformly over the lower half and cooled by maintaining a constant wall temperature over the upper half has been investigated.

The same kind of oscillatory and reverse flow motions that have been experimentally found in toroidal loops has been numerically observed. All these findings have been demonstrated numerically by brute force integration of the complete Navier-Stokes equations.

It has been also demonstrated that in laminar regions theoretical correlation eq. (7) gives good results in establishing the validity of the dimensionless group proposed by Vijayan [12, 13].

Acknowledgments

The authors acknowledge the help of R. Spampinato with some of the computational work. The support by the French National Institute for Advances in Scientific Computations (IDRIS-Computer Center) project no. 03 1265 is gratefully acknowledged.

References:

[1] Cadiou P., Desrayaud G. & Lauriat G., Natural convection in a narrow horizontal annulus: the effects of thermal and hydrodynamic instabilities, *ASME J. Heat transfer,* Vol. 120, 1998, pp. 1019-1026.

[2] Cammarata G., Desrayaud G. Fichera A. & Pagano A., An ordinary differential model for rectangular natural circulation loops, - *12th International Heat Transfer Conference (Grenoble, France),* Vol. 2, 2002, pp. 273-278.

[3] Creveling H.F., De Paz J.F., Baladi J.Y. & Schoenhals R.J., Stability characteristics of a single phase free convection loop, *J. Fluid Mech.,* Vol. 67, part 1, 1975, pp. 65-84.

[4] Desrayaud G., Fichera A. & Marcoux M., Numerical investigation of natural circulation in a 2D-annular closed-loop, *Int. J. Heat Fluid Flow,* 2005, in press

[5] Fichera A. & Pagano A., Modeling and control of rectangular natural circulation loops, *Int. J. Heat Mass transfer*, Vol. 46, 2003, pp. 2425-2444.

[6] Greif R., Natural circulation loops, *ASME J. Heat transfer,* Vol. 110, 1988, pp. 1243-1258.

[7] Huang, B.J. and Zelaya, R. Heat transfer behaviour of a rectangular thermosyphon, *ASME J. Heat transfer,* Vol. 110, 1988, pp. 487-493.

[8] Keller J., Periodic oscillations in a model of thermal convection, *J. Fluid Mech.,* Vol. 26, part 1, 1966, pp. 599-606.

[9] Lavine S., Greif R., Humphrey J.A., A three-dimensional analysis of natural convection in a toroidal loop - The effect of Grashof number, *Int. J. Heat Mass Transfer,* Vol. 30, 1987, pp.251-261.

[10] Malkus, W.R.V., Non-periodic convection at high and low Prandtl number, *Mem. Soc. R. Sci. Liege* 4kk, 1972, pp. 125-128.

[11] Misale, M., Frogheri, M., Ruffino, P. and D'Auria, F. Steady state and stability behavior of a single-phase natural circulation loop, - *11th Int. Heat Transfer Conference (Kyongju, Korea),* Vol. 3, 1998, pp. 385-390.

[12] Vijayan, P.K. Experimental observations on the general trends of the steady state and stability behaviour of single-phase natural circulation loops, *Nucl. Engng. Design,* Vol. 215, 2002, pp. 139-152.

[13] Vijayan, P.K. and Austregesilo, H., Scaling laws for single-phase natural circulation loops, *Nucl. Engng. Design,* Vol. 152, 1994, pp. 331-347.

[14] Welander P., On the oscillatory instability of a differentially heated fluid loop, *J. Fluid Mech.,* Vol. 29, part 1, 1967, pp. 17-30.

[15] Zvirin, Y., A review of natural circulation loops in Pressurized Water Reactors and other systems, *Nucl. Engng. Design,* Vol. 67, 1981, pp. 203-225.

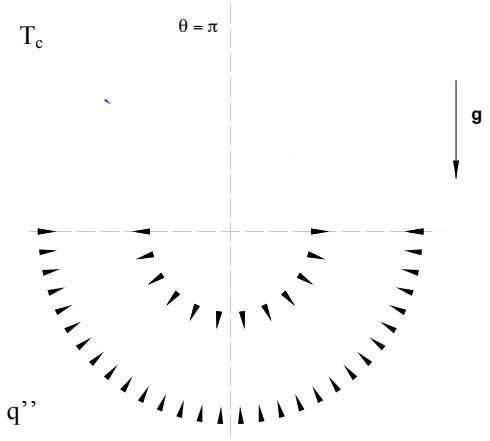

Figure 1: 2D- annular geometry

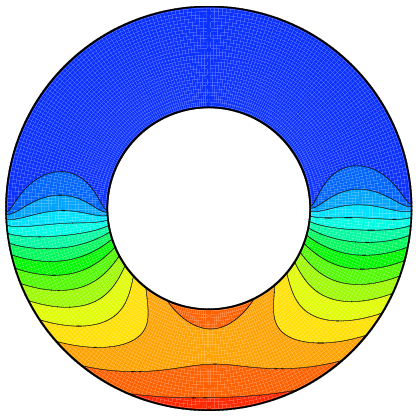

Figure 2: Temperature field, Ra = 1, R = 2.0, Pr = 5

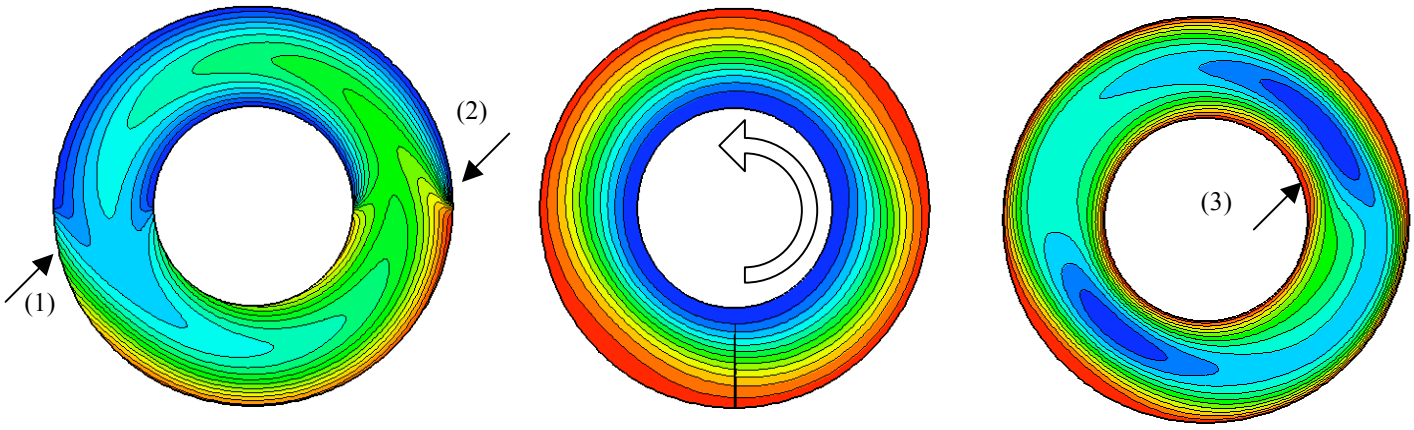

a) Isotherms **b)** Stream function **c)**Axial velocity

Figure 3: Steady motion, Ra = 10 000, R = 2.0, Pr = 5

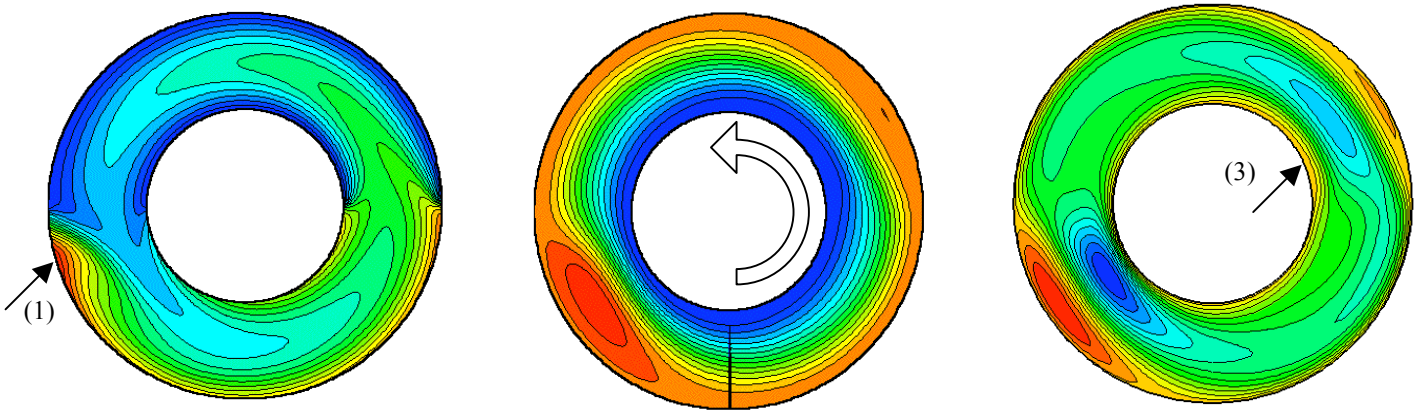

a) Isotherms **b)** Stream function **c)** Axial velocity

Figure 4: Steady motion, Ra = 13 500, R = 2.0, Pr = 5

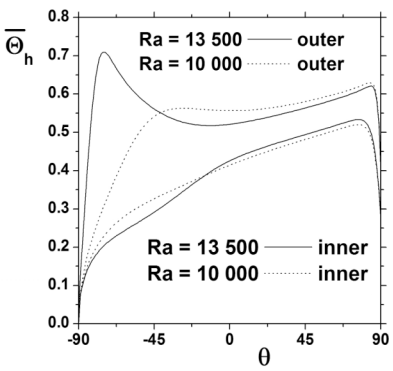

a) Inner and outer wall temperature at the heater

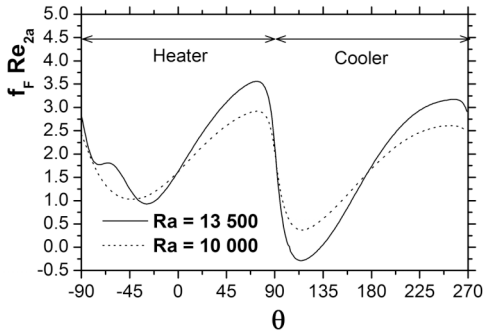

b) Local friction factor

Figure 5: Steady motion, R = 2.0

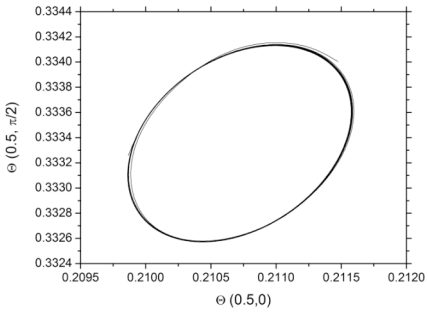

Limit cycle

Figure 6: Ra = 13 830, R = 2.0

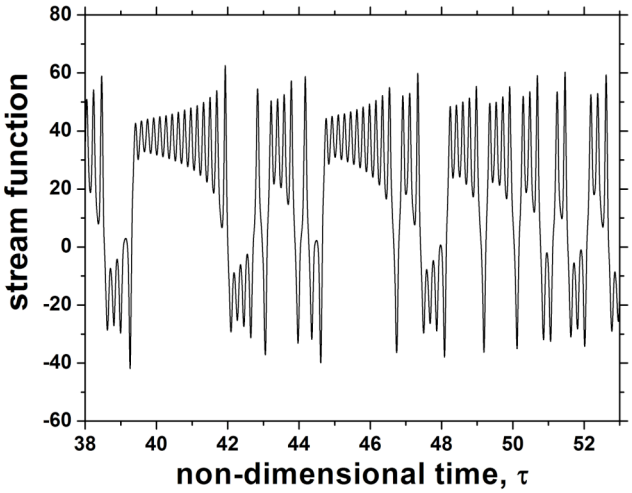

a) Time history

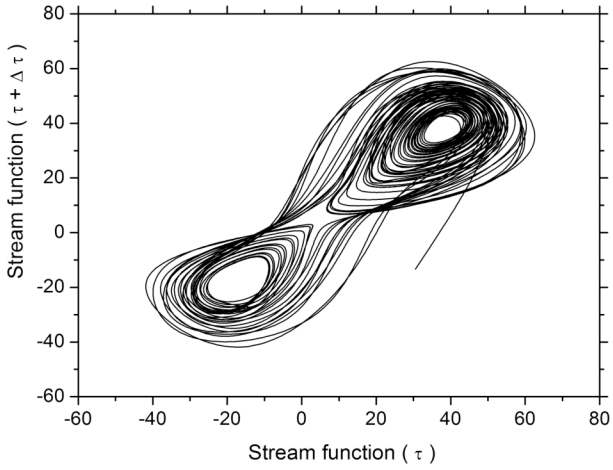

b) Lorenz attractor

Figure 7: Reverse flow and Lorenz-like attractor, Ra = 15 000, R = 2.0, Pr = 5

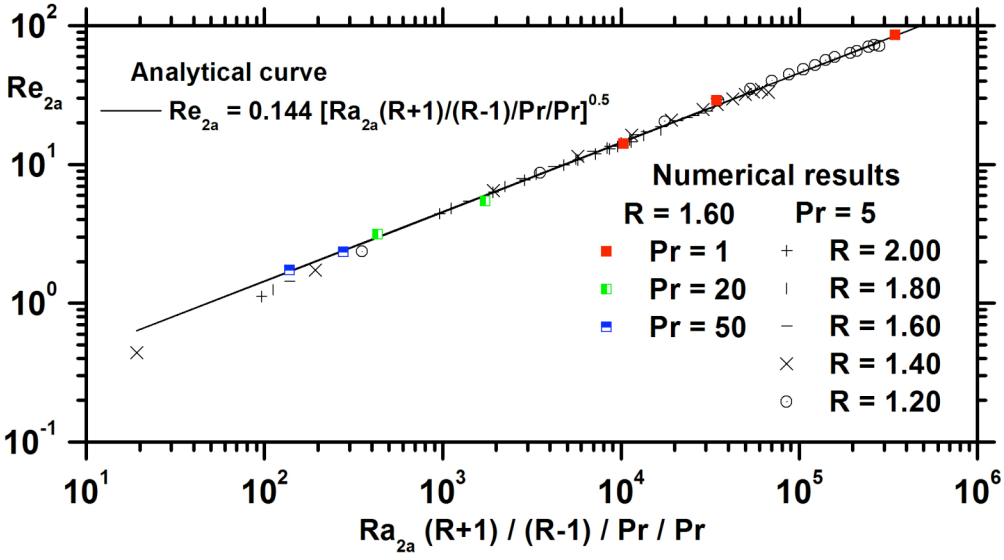

Figure 8: Evolution of the Reynolds number for various radius ratios